Effect of diffuser inlet width on cantilever multistage centrifugal pump

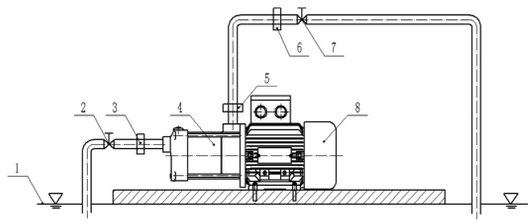

Efecto del ancho de la entrada al difusor en bomba centrifuga multietapa en voladizo

Jiang Xiaoping[1], Wang Chuan[1,2*], Wu Jiahui[1], Shi Weidong[1], Liu Sihan[1] and Yang Yongfei[1]

[1] National Research Center of Pumps & Pumping System Engineering & Technology, Jiangsu University, Xuefu Road 301#, Zhenjiang, 212013, Jiangsu, China, wangchuan198710@126.com
[2] Maritime Research Centre, Nanyang Technological University, 50 Nanyang Avenue, 639798, Singapore.

DOI: http://dx.doi.org/10.6036/8153 | Recibido: 12/09/2016 • Aceptado: 22/11/2016

ABSTRACT

• Five diffusers with different axial widths were constructed based on the area ratio principle to solve the problem that axial dimension errors of impeller and diffuser strongly affect the external performance and internal flow of a cantilever multistage centrifugal pump. Field calculations on a two-stage centrifugal pump were performed using the RNG k-ε turbulence model on ANSYS Computational Fluid X. External characteristic experiments were also conducted to benchmark the numerical calculation. The external performance and velocity distribution in the different pump models were determined. Results show that when the diffuser inlet width is less than the impeller outlet width, an increase in the diffuser inlet width always causes a reduction in the pump head, and the pump efficiency increases at a small flow rate but decreases at a large flow rate. When the diffuser inlet width is larger than the impeller outlet width, the pump head and efficiency decrease constantly, and the rate of decrease increases gradually. The core zone and turbulent boundary exist in the front pump cavity. With an increase in the diffuser inlet width, the non-dimensional circumferential component velocity in the core zone reduces gradually, the effect of turbulent boundary on the flow in the core zone weakens slowly, and the non-dimensional radial component velocity is always approximate to zero. This study provides a new reference for the matching design between impeller and diffuser.

• **Keywords:** Multistage centrifugal pump, inlet width, diffuser, front pump cavity.

RESUMEN

Se construyeron cinco difusores con diferentes anchos axiales basándose en el principio de proporción de área, para resolver el problema de que los errores de dimensión axial de rodete y difusor afecten fuertemente al funcionamiento externo y al flujo interno de una bomba centrífuga cantilever multietapa. Se realizaron cálculos de campo en una bomba centrífuga de dos etapas utilizando el modelo de turbulencia RNG k-e mediante el programa informático ANSYS-Fluid X. También se realizaron experimentos externos para contrastar el cálculo numérico. Se determinaron el rendimiento externo y la distribución de velocidad en diferentes modelos de bomba. Los resultados muestran que cuando la anchura de entrada del difusor es menor que el ancho de la toma del rodete, un aumento en la anchura de entrada del difusor siempre causa una reducción en la altura de presión de la bomba y la eficiencia de la bomba aumenta con un caudal pequeño pero disminuye con un gran caudal. Cuando el ancho de entrada del difusor es mayor que el ancho de salida del rodete, la altura de presión de la bomba y la eficiencia disminuyen constantemente y la tasa de disminución aumenta gradualmente. En la cavidad frontal de la bomba coexiste una zona interna y una periférica turbulenta. Con un aumento en la anchura de entrada del difusor, la velocidad del componente circunferencial adimensional en la zona interna se reduce gradualmente, el efecto de la periferia turbulenta en el flujo donde la zona interna disminuye poco a poco y la velocidad del componente radial adimensional siempre se aproxima a cero. Este estudio proporciona una nueva referencia para el diseño equilibrado entre rodete y difusor.

Palabras clave: Bomba centrífuga multietapa, ancho de entrada, difusor, cavidad frontal de bomba.

1. INTRODUCTION

Cantilever multistage centrifugal pump has advantages such as compact structure, easy installation, high reliability, convenient maintenance because of its very simple structure in the pump. In many fields, such as building water supply, petrochemical production, metallurgy, electric power, water conservancy, and agricultural irrigation, the traditional double-support structure of the multistage centrifugal pump is gradually replaced with the cantilever multistage centrifugal pump, and the latter is being applied widely. The multistage centrifugal pump mainly consists of an impeller and a diffuser, and the internal flows of such a pump are extremely complex [1-3]. Research has shown that the passage area ratio between the impeller outlet and the throat inlet of the diffuser is the main factor that influences the performance parameters of the multistage centrifugal pump, such as the head, flow, and axial power. As one important component part of the pump, the diffuser can convert the kinetic energy into the pressure energy of the fluids in the pump, and the conversion efficiency is influenced strongly by the match of the impeller and diffuser. However, the cantilever structure causes errors between the impeller and the diffuser to accumulate along the axial direction during installation. The accumulated errors from the design and the manufacture make the impellers and diffusers deviate from the optimal axial position, which may lead to performance reduction of the pump. Other problems caused by the accumulated errors are serious abrasion, vibration, and noise. These problems should be considered and solved.

In recent years, studies on multistage centrifugal pumps have focused on structure optimization, external performance prediction, and cavitation performance [6-11]. Wang et al. [12] simulated the entire flow field of a stainless steel punching well pump with different blade thicknesses and analyzed the influence of the blade thickness on the performance of the entire machine. Dai et al. [13] investigated the effect of the width of the single-stage impeller on the pressure fluctuation in the centrifugal pump based on experiment and numerical simulation. Considerable literature has introduced the matching state between the impeller and the diffuser. Arndt et al. [14] studied the influence of the matching of the impeller guide vane on the flow field and the performance of a centrifugal pump. Yang et al. [15] proposed a design method for the high-efficiency volute cross section of the centrifugal pump based on the principle of area ratio. However, studies on cantilever multistage centrifugal pumps remain limited. Based on the area ratio principle, five different diffusers with different axial widths are designed in this study to investigate the impeller–diffuser matching characteristic and the flow in the front pump cavity for the cantilever multistage centrifugal pump. Computational fluid dynamics (CFD) is used to explore the effect of the diffuser inlet width on the internal flow field and the external performance of the pump. This study could lay a foundation for investigating the reliability and stability of cantilever multistage centrifugal pumps.

The rest of this paper is organized as follows. Section 2 presents the five diffusers based on the area ratio principle and the setting method of numerical calculations on the multistage centrifugal pumps with different diffusers. Section 3 provides the external performance and velocity distribution in the different pump models and obtains the optimal combination of impeller and diffuser. Section 4 summarizes the results and future research directions.

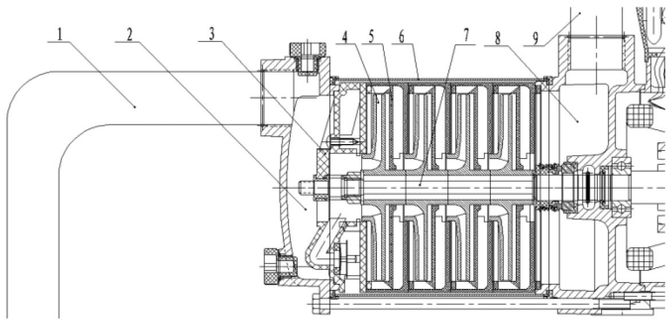

Fig. 1: Assembly diagram of cantilever multistage centrifugal pump as follows: 1. Inlet pipeline; 2. Air-water mixture cavity; 3. Self-priming plate; 4. Impeller; 5. Diffuser; 6. Outer hull; 7. Shaft; 8. Air-water separation cavity; 9. Outlet.

Geometric parameter	Value	Geometric parameter	Value
Inlet diameter of the impeller D_1 (mm)	45	Inlet diameter of the positive diffuser D_3 (mm)	104
Hub diameter of the impeller D_{hb} (mm)	20	Number of the impeller blades Z	6
Outlet diameter of the impeller D_2 (mm)	103	Rated flow Q_t (m^3/h)	10
Outlet width of the impeller blade b_2 (mm)	10	Single-stage head H (m)	8
Outlet angle of the impeller blade β_2 (°)	16	Rotating speed n (r/min)	2800
Inlet width of the positive diffuse b_3 (mm)	11	Efficiency of the pump η (%)	56.9
Width of the throat a_3 (mm)	4.6	Number of the diffuser blades z	12

Table I: Basic geometric parameters of the original pump

2. MATERIALS AND METHODS

2.1. MAIN DESIGN PARAMETERS

Figure 1 shows the stainless steel cantilever multistage centrifugal pump with the following basic design parameters as follows in Table I, and the real pump model is shown in Fig. 1.

2.2. DESIGN OF MATCHING SCHEME BETWEEN IMPELLER BLADE AND DIFFUSER BASED ON AREA RATIO PRINCIPLE

The diffuser is designed with a continuous entire flow passage from the positive diffuser to the return diffuser. This design is equipped with several flow channels from the inlet of the positive diffuser to the outlet of the return diffuser, with an interference-free characteristic among the flow channels. The flow of this type of diffuser is smoother and the hydraulic performance is better than those of the radial diffuser. The main geometric parameters of the positive diffuser can be seenin Table I, and based on the area ratio principle of centrifugal pump, the area ratio coefficient of the cantilever multistage centrifugal pump is defined as follow

$$Y = \frac{F_3}{F_2} = \frac{\text{Total area of the guide vane inlet}}{\text{Total area of the impeller outlet}} \tag{1}$$

$$F_2 = \pi D_2 b_2 \tan \beta_2 \tag{2}$$

$$F_3 = z a_3 b_3 \tag{3}$$

Therefore, the coefficient of cantilever multistage pump area ratio is

$$Y = \frac{F_3}{F_2} = \frac{z a_3 b_3}{\pi D_2 b_2 \tan \beta_2} \tag{4}$$

According to Equation (4), if the impeller parameters, the number of positive diffuser z, and the width of the throat a_3 are determined, then the area ratio coefficient Y is proportional to the inlet width b_3.

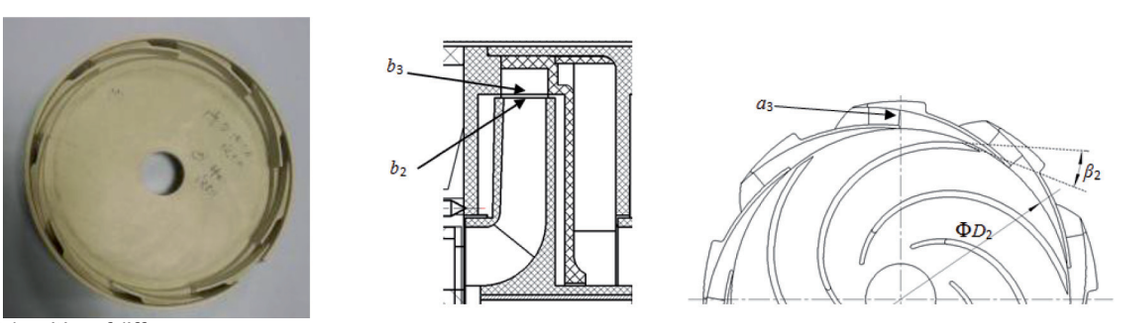

Fig. 2: Flow channel and axial position of diffuser

The preliminary parameters for the diffuser of the cantilever multistage centrifugal pump are shown in Figure 1. The same impeller is matched with the positive diffusers with varying inlet widths (namely, different area ratios) to study and solve the negative effect on the pump performance caused by the axial displacement of the impeller and diffuser and to reduce the possible effect of grinding, vibration, and noise. Then, the numerical calculation method is used to determine the optimal matching relationship. When the model is assembled, the inlet width b_3 of the positive diffuser is set as 9, 10, 11, 12, and 13 mm, and each setting is matched with the same impeller with outlet width $b_2 = 10$ mm, through which the axial size of the back pump cavity formed by the position of the impeller hub and diffuser remains unchanged. The axial size of the front pump cavity b_4 changes with the diffuser inlet width b_3 (see Figure 2), and the area ratio Y changes correspondingly.

2.3. MODEL ESTABLISHMENT

Multistage centrifugal pumps are more complicated than single-stage centrifugal pumps. The swirling of the inlet flow of the impellers, except for the first one, is caused by the outlet flow of diffusers. Moreover, the efficiency of the first stage differs significantly from that of other stages. The number of stages should be determined first to improve the calculation accuracy. In the cantilever multistage pump in this study, b_2 and b_3 are set as b_2 = 10 mm, b_3 = 11 mm and the pumps for the first four stages are simulated numerically under the design condition. The results of the simulations for the efficiency at each stage are shown in Table II.

Stage number *n*	1	2	3	4
Efficiency of the first stage pump (%)	59.59%	60.09	59.98	59.02
Efficiency of the second stage pump (%)		57.58	57.54	57.61
Efficiency of the third stage pump (%)			57.88	57.76
Efficiency of the fourth stage pump (%)				57.91
Total efficiency (%)	55.66	56.97	57.43	57.36

Table II: Efficiency comparison of different stages

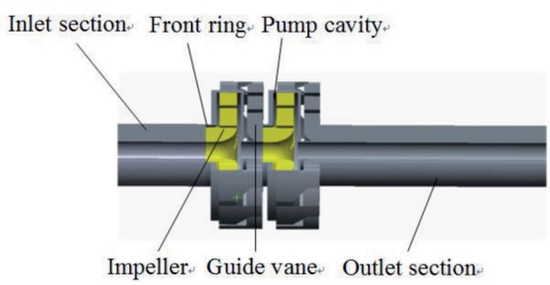

Fig. 3: Calculation model of a two-stage pump

Table II shows that the efficiency of the first stage is relatively large, whereas the efficiency of the second stage is near that of the later stages, which verifies that the flow is irrotational in the first stage but rotational in the other stages. In consideration of the computer resource requirement, which increases with an increase in the stage number, the entire flow field model for two stages is established for this study, and the second-stage efficiency is used to predict the performance value. As shown in Figure 3, the entire flow field domain with two stages is modeled using Creo 2.0 software. The inlet and outlet sections of the water domain are extended properly to avoid the backflow phenomenon in the inlet and outlet.

2.4. MESH GENERATION

To generate a high-quality structured mesh for the water body, ICEM software is used and the mesh near the boundary layer is refined. As shown in Fig. 4, the calculation domain consists of six parts, namely, inlet section, mouth ring, impeller, pump cavity, diffuser, and outlet section. The mesh quality directly affects the calculation accuracy. Compared with the unstructured mesh, the structured mesh has better quality and is faster to generate, thereby increasing the calculation accuracy and reducing the calculation time.

As the calculation results depend on the mesh density and quality, testing the mesh independence and ensuring the quality of each flow field to be greater than 0.30 are necessary. Meshes with four different cell numbers are used for the grid independence study. The head values calculated from each case are compared, as shown in Table III. Among them, the difference in the predicted head values between cases *A* and *B* is 5.03%, whereas the deviations in cases *B*, *C*, and *D* are 1.52%, 1.85% and 0.33%

Case	Mesh numbers×10^6	Efficiency/%
A	0.85	60.76
B	1.86	57.85
C	2.34	56.97
D	3.81	56.78

Table III: Inspection of grid independence

respectively. With regard to the calculation time and coordination accuracy, when the total number of mesh elements is 2,340,000, the calculation requirements are not met.

2.5. SELECTING THE TURBULENCE MODEL

In this study, numerical calculations were performed with ANSYS CFX software, which provides a number of turbulence models.

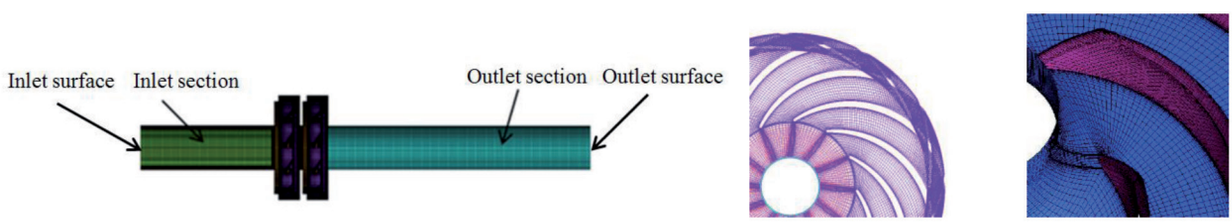

(a) *(b)* *(c)*

Fig. 4: Structured mesh of fluid entire flow field. (a) Entire domain. (b) Diffuser domain. (c) Impeller domain

Turbulence model	Standard k-ε	RNG k-ε	BSL k-ω	Standard k-ω	SST k-ω	Test value
Efficiency η (%)	57.28	56.97	59.34	59.57	59.91	55.89

Table IV: Numerical and experimental results with different turbulent models under rated flow condition

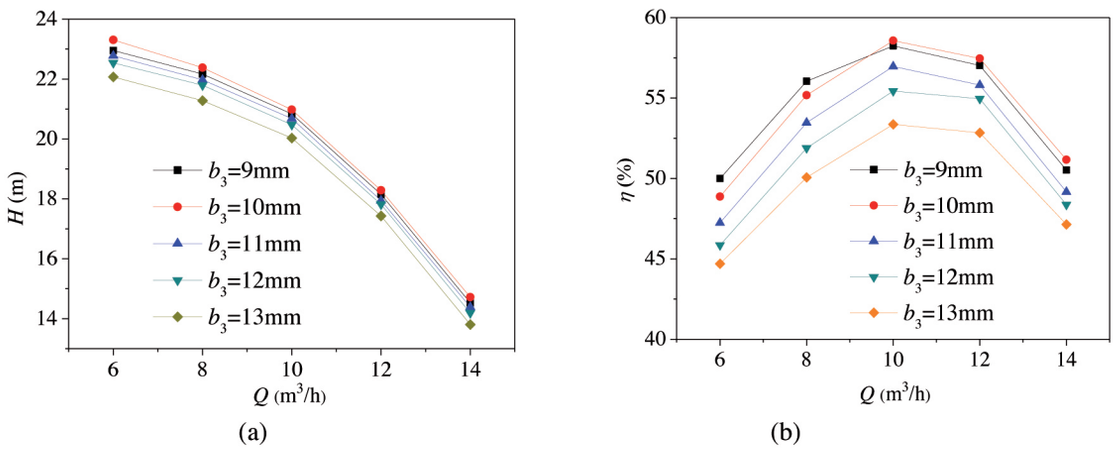

Fig. 5: Performance curve of model pumps. (a) H-Q .(b) η-Q

Among the turbulence models, *k*-ε and *k*-ω are known to be the most suitable for the internal flow of rotating machines. Therefore, five models, i.e., Standard *k*-ε, RNG *k*-ε, BSL *k*-ω, Standard *k*-ω, and SST *k*-ω, were selected, and their results were compared with the experimental results. Table IV shows that the prediction by RNG *k*-ε model is closest to the experimental data; thus, this model was selected in this study.

2.6. BOUNDARY CONDITION

The mesh generated through ICEM is imported in ANSYS Computational Fluid X (CFX) 14.5 to conduct the solving process. The inlet and outlet boundary of the calculation domain are the velocity inlet and free outflow respectively.The surface roughness is set to 25 μm. The rotating coordinate system is adopted in the flow field of the impeller, and the rotation speed is 2800 r/min. The rest of the flow field is set to a stationary coordinate system. As the impeller of the multistage pump and the flow passage type diffuser are composed of a curved wall surface, the streamline has a large bending degree, and the Reynolds stress has obvious anisotropy. The RNG *k*-ε turbulence model comprises the continuity equation and the Navier–Stokes equation that forms a closed set of equations. With this model, the turbulent fully developed region can be predicted efficiently. In the calculation, the head and average static pressure of the inlet and outlet sections of the multistage pump are monitored. The average residual is calculated as the convergence criterion, and the residual value is set to 10^{-5}.

3. RESULT ANALYSIS AND DISCUSSION

3.1. COMPARISON OF EXTERNAL CHARACTERISTICS

Under the given settings, the five different diffuser models are simulated by ANSYS CFX. The performance curve of the pump with different inlet widths of the positive diffuser is obtained, as shown in Figure 5.

Figure 5(a) exhibits the curve of head and flow rate. Under the same flow condition, the head of the pump model with b_3 = 10 mm is the highest, whereas that with b_3 = 13 mm is the lowest. The head first increases and then decreases with the width of the diffuser varying from 9 mm to 13 mm. From the $0.6Q_{sp}$ to the $0.8Q_{sp}$ working condition, the head is sensitive to the change in the inlet width. In particular, when the width increases from 12 mm to 13 mm, the head difference value reaches the maximum with a value of 0.31 m. From the $1.0Q_{sp}$ to the $1.4Q_{sp}$ working condition, the head difference of the model pump is small, and it decreases with an increase in the flow rate. Therefore, the influence of the positive diffuser inlet width (namely, the area ratio of the impeller and the diffuser Y_1) on the head is reduced gradually with an increase in the flow rate.

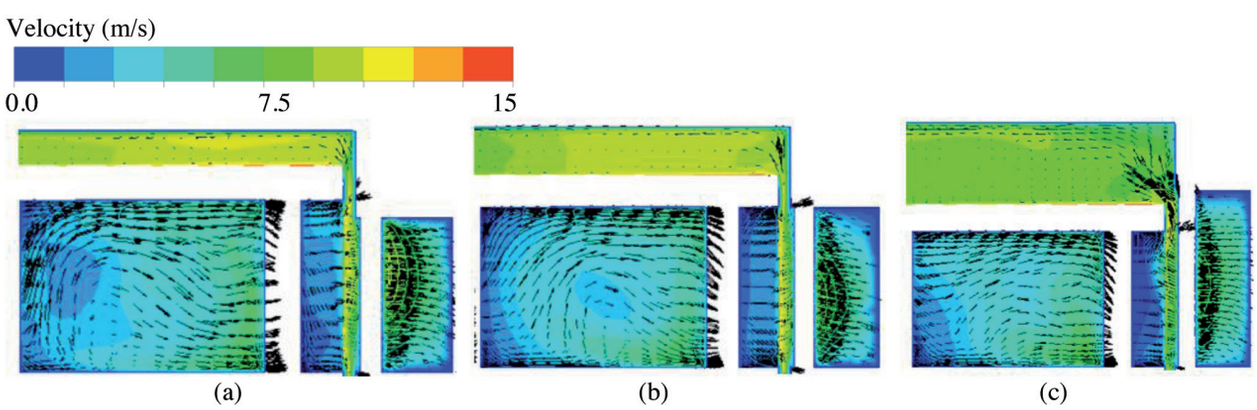

Fig. 6: Meridian velocity vector and contour. (a) b_3 = 9 mm. (b) b_3 = 10 mm. (c) b_3 = 13 mm

Figure 5(b) indicates that, with the increase of the diffuser inlet width, the pump efficiency under rated flow condition and large flow condition increases first and then decreases, finally reaches the highest value when b_3 = 10 mm. However, under the small-flow-rate condition, the efficiency of the model pump decreases with an increase in the inlet width. The pump efficiency almost keeps stable when the diffuser inlet width varies from 9 mm to 12 mm. By contrast, the pump efficiency decreases rapidly, especially in the rated condition, when the width exceeds 12 mm. Accordingly, the width of the diffuser inlet has a strong influence on the pump performance. When the width of the diffuser inlet is different under the same flow rate, the maximum values of the efficiency difference and the head difference are 7.53% and 7.70%, respectively. The preceding discussion indicates that for the multistage centrifugal pump, especially the cantilever multistage pump, the width of the positive diffuser inlet should be located within a suitable range.

3.2. ANALYSIS OF INTERNAL FLOW CHARACTERISTICS

The reasons for the increase of the head and efficiency when b_3 = 10 mm and their rapid decline when b_3 = 13 mm under the rated-flow condition are analyzed. Figure 6 presents the meridian velocity vector diagram and the velocity contour of the transition zone between the secondary impeller and the diffuser under the rated-flow condition for b_3 = 9,10,13 mm. The internal flow of the diffuser model is relatively regular, and an obvious low-velocity zone exists between the impeller outlet and the diffuser inlet. The diffuser converts the velocity energy into the pressure energy, which forms a large pressure gradient for the surrounding fluid. The low-velocity area increases with an increase in the diffuser inlet width. The velocity vector indicates that within the three types of inlet width, the impeller internal flow pattern is best in the model with b_3 = 10 mm.

When b_3 = 9 mm, as shown in Figure 6(a), part of the impeller flow channel outlet is blocked by the limited flow area because the width of the impeller outlet (10 mm) is larger than that of the width of the diffuser inlet (9 mm). The capability of flow channel diffusion is reduced, which leads to an increase of nonuniform flow in the impeller outlet. In the diffuser inlet, turbulent dissipation and significant water shock loss occur. A large residual vortex appears in the region near the suction surface of the middle part of the impeller. As a result, large hydraulic loss is produced, and the nonuniformity of the outflow can also have a significant influence on the pressure pulsation and vibration excitation. When the diffuser inlet width increases to 13 mm, the head and efficiency of the model pump decrease rapidly. The main cause of this phenomenon is that the width of the diffuser inlet is higher than that of the impeller outlet, and the fluid is thrown out and flows into the diffuser because of the impeller rotation. The velocity in the diffuser inlet is higher than that in the impeller outlet because of the area difference of the flow channels. Moreover, the secondary backflow is formed between the diffuser and the front pump cavity, thereby resulting in a large hydraulic loss in the pump, as shown in Figure 6(c). Given that the pump cavity is filled with fluid, when the impeller rotates, a disc friction loss occurs between the fluid and the cover plate of the impeller. With an increase in the width b_3, the impeller position does not change, thereby resulting in an inevitable increase in b_4, which is the clearance of the front pump cavity between the front cover of the impeller and the face of the front stage diffuser. The larger the value of b_4, the more fluid is in the pump cavity gap. Therefore, considerable hydraulic loss occurs in the pump cavity circulation. The efficiency is high and the head drop of the model pump is fast when b_3 = 13 mm.

3.3. FLOW FIELD CHARACTERISTICS OF FRONT PUMP CAVITY

According to the preceding analysis, the influence of the diffuser inlet width b_3 on the external characteristics of the multistage centrifugal pump is closely related to the flow characteristics of the fluid in the front pump cavity. Taking the front pump cavity before the secondary impeller as an example, this paper discusses the flow characteristics of the fluid in the front of the pump cavity under different inlet width conditions of the diffuser. Given space limitations, this section analyzes the flow fields of the front pump cavity under the rated condition when the diffuser inlet width b_3 is 9, 10, and 13 mm.

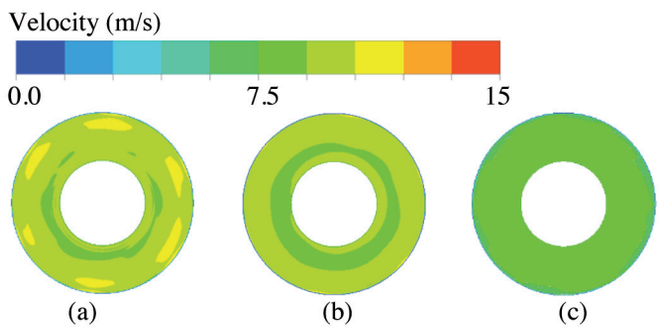

Fig. 7: Velocity distribution in front cavity. (a) b_3 = 9 mm. (b) b_3 = 10 mm. (c) b_3 = 13 mm

Affected by the symmetrical flow of diffusers, the velocity distribution of the fluid that is rotating in front of the pump cavity is also symmetrical. Figure 7 shows the velocity distribution in the central axial section of the front pump cavity with different inlet widths. Under the rated-flow condition, the flow velocity of the fluid in the front pump cavity first increases and then decreases along the radial direction. The change is relatively uniform. Owing to the combined effect of radial leakage flow that exists in the ring clearance and the rotation of the front cover plate of the impeller, the value of the pressure gradient and the velocity of the fluid decrease (the minimum velocity value is up to 1 m/s) at the position of a larger radius. When b_3 increases from 9 mm to 10 mm and then to 13 mm, the average velocity of fluid in the front pump cavity continues to decrease. The absolute velocity when b_3 is 13 mm is obviously smaller than that when b_3 is 9 mm, which indicates that the core rotation zone exists between the rotating front cover plate and the static wall. The effect of the rotating front cover plate on the core area decreases with an increase in the diffuser inlet width.

The circumferential and radial flow characteristics of the fluid in the front pump cavity are studied; thus, the effect of b_3 and b_4 on the flow characteristics in the front of the pump cavity can be further discussed. Figures 8 and 9 show the non-dimensional circumferential velocity and the non-dimensional radial velocity distribution of the monitoring points that are located in the three circles on the velocity distribution photos of the front pump cavity with radii of 0.6, 0.8, and 1.0 R along the axial direction, respectively. The non-dimensional circumferential velocity represents the ratio of circumference velocity component v_u against the impeller rotational velocity w_u at the monitoring point. The non-dimensional radial velocity component represents the ratio of the radial velocity v_r against the impeller rotational velocity w_r at the monitoring point. S represents the distance between the monitoring point and the static wall surface, δ is the thickness of

the front pump cavity, and *R* is the radius of the impeller. The fluid flow in the front pump cavity is axially symmetric; thus, any of the axial sections in the pump cavity could be selected.

Figures 8(a) to 8(d) illustrate that the front pump cavity has a core flow region where the non-dimensional circumferential velocity is almost unchanged under the rated-flow condition. The comparison of three kinds of inlet width shows that with the increase of the pump cavity thickness, the axial length of the core flow region increases, and the core region becomes closer to the static wall of the diffuser. Furthermore, the non-dimensional cir-

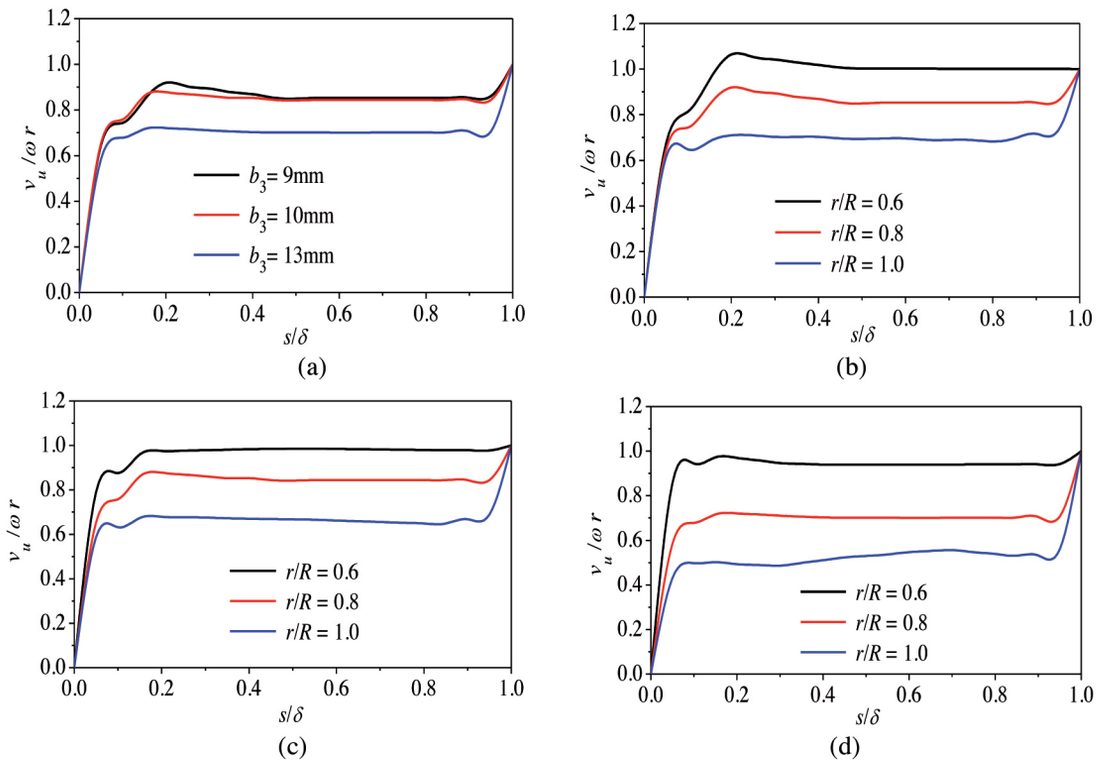

Fig. 8: Axial distribution of circumferential velocity. (a) 0.8 R. (b) b_3 = 9 mm. (c) b_3 = 10 mm. (d) b_3 = 13 mm

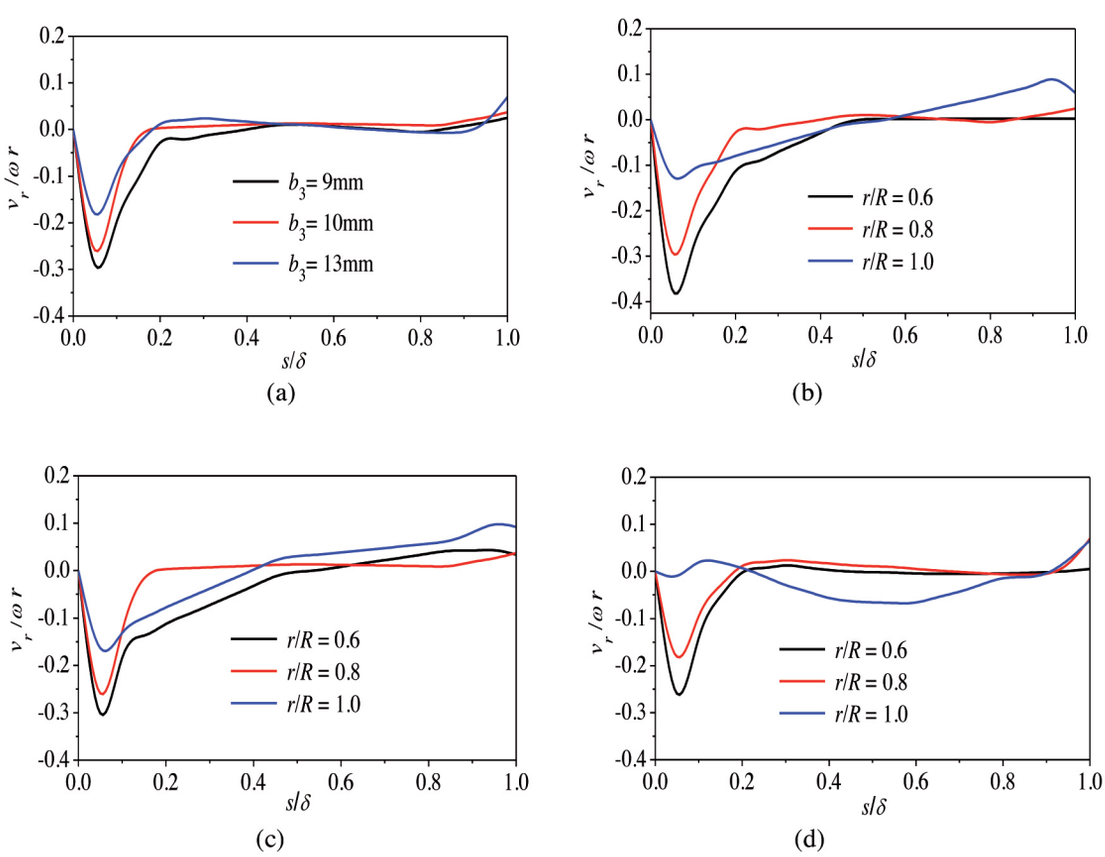

Fig. 9: Axial distribution of radial velocity. (a) 0.8 *R. (b) b_3* = 9 mm. *(c) b_3* = 10 mm. *(d) b_3* = 13 mm

cumferential velocity is larger near the shroud of the impeller, and the non-dimensional circumferential velocity is small where it is close to the static wall. In the same axial section, with an increase in r/R, the dimensionless circumferential velocity of the core region decreases gradually. In the core area where the diameter is 0.6 R, the non-dimensionless circumferential velocity is larger with a value of almost 1. According to the analysis, such a phenomenon is mainly caused by the leakage flow of the ring clearance. When the high-energy fluid flows from the impeller outlet to the front of the pump cavity, the fluid with a higher velocity transfers the energy to the fluid where the position is at a small radius because of the viscous force effect. Figure 8(a) also shows that when b_3=9 mm or 10 mm, the difference in the non-dimensional circumferential velocity component is small at 0.8 R. When b_3 increases to 13 mm, the non-dimensional circumferential velocity decreases significantly, because the increase in the pump cavity axial clearance weakens the mutual interference of the core area flow and boundary layer flow.

The non-dimensional radial velocity distribution of the diffuser with different inlet widths along the axial direction at a radius of 0.8 R is shown in Figure 9(a). A core flow area remains in the pump cavity, but the general trend decreases. As shown in Figures 9(b) to 9(d), at the same radial position in the pump cavity with different axial widths, the non-dimensional radial velocity along the axial direction first decreases and then increases gradually after reaching the minimum value. Thereafter, the value stabilizes at approximately 0 because the pump cavity flow is mainly composed of the core area flow and boundary layer flow. The fluid near the rotating impeller front cover is influenced by the "pump capacity" of the rotary impeller cover. Given that the centrifugal force overcomes the force caused by the radial pressure difference, the fluid flows to the outer diameter. Nevertheless, the radial velocity component is smaller than the absolute velocity of the cover plate that leads to a small non-dimensional radial velocity in the impeller front cover wall surface.

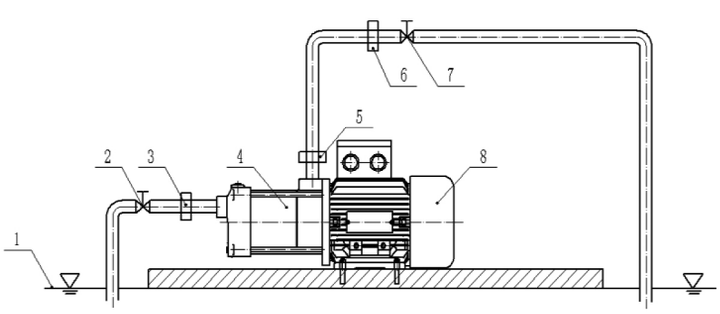

Fig. 10: Schematic diagram of the test rig: 1. Pool 2. Inlet control valve 3. Inlet pressure transmitter 4. Pump 5. Outlet pressure transmitters 6. Turbine flowmeter 7. Flow control valve 8. Motor

At the side close to the static wall, the angular velocity produced by the fluid is too small to overcome the radial pressure difference induced by the ring leakage. Consequently, a negative non-dimensional radial velocity exists near the wall surface. With an increase in the axial clearance of the pump cavity, the absolute value of the non-dimensional radial velocity decreases. When the width of b_3 is 13 mm, the minimum value is 0.26. The radial velocity of the fluid in the core region is relatively small in relation to the boundary layer, and no radial flow basically exists. When b_3 is 13 mm and r/R=1.0, the dimensionless radial velocity in the same position is obviously different from that when b_3 is 9 or 10 mm, indicating that the non-uniform distribution of the radial flow field velocity appears at the outer diameter when the diffuser inlet is larger than the impeller outlet width.

3.4. EXPERIMENTAL VERIFICATION OF PUMP MODELS

Two groups of pump model with the diffuser width of b_3 = 11 mm (original model) and b_3 = 10 mm (optimal model) are converted into a prototype to verify the actual reliability of the numerical calculation. The simulations were performed at five flow points (Q = 1.65, 2.64, 3.3, 3.96, 5.4 m^3/h). At the same time, the hydraulic models were shown to a pump company in Fujian Province, and a five-stage centrifugal pump was manufactured. Then, the pump was sent to the National Water Pump and System Engineering Technology Research Center of Jiangsu University for performance testing. As shown in Figure 10, the test rig is an open-type system, which is composed of two parts—acquisition and water circulation systems. A turbine flowmeter was used to measure the flow rate Q with a precision of ±0.3%. The pump speed n was measured by a tachometer (PROVA RM-1500, Taiwan) with a precision of ±0.04%. During the experiment, two pressure transmitters (CYG1401, China) with a precision of ±0.2% were used to measure the inlet and outlet pressures.

The comparisons between the numerical and experimental results are presented in Figure 11. The efficiency curves of the numerical and experimental results are nearly the same in the trend. Under the rated flow condition and large flow rate conditions, the numerical and experimental values present an insignificant difference and have a good agreement. The error under the rated-flow condition is within 3%. Under the small flow condition, the calculated value is significantly higher than the experimental values, and their error is large. According to the analysis, given that the pump operates under the small-flow-rate condition, flow separation and shock phenomenon are prone to appear in the flow components and result in large hydraulic loss, but the error is less than 3%. Thus, the numerical prediction has relatively high accuracy. The results show that the performances of the pump can be credibly predicted using CFD through the entire calculation model and appropriate numerical setting method.

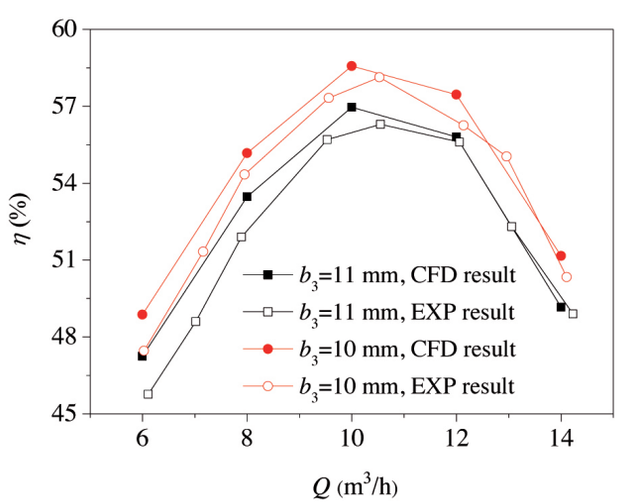

Fig. 11: Comparisons between the numerical and experimental results

4. CONCLUSIONS

In this study, five groups of three-dimensional CFD simulations are conducted to analyze the effect of axial errors between

the impeller and the diffuser on the external characteristics and the internal flow of a cantilever multistage centrifugal pump. The conclusions drawn from this study are as follows:

(1) The diffuser inlet width that is smaller than the impeller outlet width results in a low pump head. With an increase in the diffuser inlet width, the efficiency increases under the small-flow-rate condition but decreases under the large-flow-rate condition. By contrast, the head and efficiency decrease with an increase in the diffuser inlet width, and the decreasing rate becomes significant when the diffuser inlet width increases to 13 mm.

(2) The low-velocity zone exists in the transition section from the impeller to the diffuser in the different models. The low-velocity zone is more obvious in the diffusers with a larger inlet width. When the diffuser inlet width is small, the trapped vortex appears in the impeller center near the suction surface area. The secondary back flow forms easily between the diffuser and the pump cavity in the models with a large inlet width.

(3) The flow field in the front pump cavity is symmetric, and the core area and the turbulent boundary layer exist in the middle of the pump cavity. The boundary layer of the turbulent flow is strongly affected by the leakage of the front ring. With an increase in the diffuser inlet width, the turbulence boundary has a weaker effect on the core flow region.

(4) The accumulated errors from the design and the manufacture may make the impellers and diffusers deviate from the optimal axial position, which may lead to performance reduction of the pump. Firstly, the diffuser inlet width should not be smaller than the impeller outlet width so that the pump performance keeps stable. Secondly, it's best to make the central plane of the impeller coincide with that of the positive diffuser to keep a high efficiency. Thirdly, it's very necessary to check the axial position of the impeller before running.

This paper only presents the experimental results of the optimal pump model. In the next step, different numerical models should be processed with the real experimental models to verify the accuracy of numerical calculations completely. Moreover, vortex distribution, as an important flow characteristic in the pump, should be considered in future studies.

BIBLIOGRAPHY

[1] Zhou L, Shi W D, Li W, et al. "Particle Image velocimetry measurements and performance experiments in a compact return diffuser under different rotating speed". Experimental Techniques. February 2016. Vol 40-1. p.245-252. DOI: http://dx.doi.org/10.1007/s40799-016-0028-6.

[2] Hydraulic Institute, Europump and US-DOE, 2004. "Variable speed pumping: a guide to successful applications". Hydraulic Institute, New York, NY.

[3] Hergt P H. "Pump research and development: past, present, and future". Journal of Fluids Engineering, January 1999. Vol 121-2. p.248-253. DOI: http://dx.doi.org/10.1115/1.2822198.

[4] Ouchbel T, Zouggar S, Elhafyani M L, et al. "Power maximization of an asynchronous wind turbine with a variable speed feeding a centrifugal pump". Energy Conversion and Management. February 2014. Vol 78-1. p.976-986. DOI: http://dx.doi.org/10.1016/j.enconman.2013.08.063. 2014, 78-2: 976-984.

[5] Goto A, Nohmi M, Sakurai T, et al. "Hydrodynamic design system for pumps based on 3-D CAD, CFD and inverse design method". ASME Journal of fluids Engineering. February 2002. Vol 124-2. p.329-335. DOI: http://dx.doi.org/10.1115/1.1467599.

[6] Park J H, Kim C G, Lee Y H. "Efficient energy storage method by multistage pump of the energy storage system using CFD". International Journal of Energy Research. October 2015. Vol 40-5. p.685-691. DOI: http://dx.doi.org/10.1002/er.3432.

[7] Suh S H, Rakibuzzaman, Kim K W, et al. "A study on energy saving rate for variable speed condition of multistage centrifugal pump". Journal of Thermal Science. November 2015. Vol 24-6. p.566-573. DOI: http://dx.doi.org/10.1007/s11630-015-0824-9.

[8] Sedlář M, Krátký T, Zima P. "Numerical analysis of unsteady cavitating flow around balancing drum of Multistage Pump". International Journal of Fluid machinery & systems. April 2016. Vol 9-2. p.119-128. DOI: http://dx.doi.org/10.5293/IJFMS.2016.9.2.119.

[9] Barrio R, Fernández J, Blanco E, et al. "Estimation of radial load in centrifugal pumps using computational fluid dynamics". European Journal of Mechanics - B/Fluids. May 2011. Vol 30-3. p.316-324. DOI: http://dx.doi.org/10.1016/j.euromechflu.2011.01.002.

[10] Murugesan C, Rudramoorthy R. "Numerical and experimental study of single stage and multistage centrifugal mixed flow submersible borewell pumps". International Journal of Fluid Machinery & Systems. April 2016. Vol 9-2. p.107-118. DOI: http://dx.doi.org/10.5293/IJFMS.2016.9.2.107.

[11] Rakibuzzaman, Suh S H, Kim H H, et al. "Cavitating Flow Analysis of Multistage Centrifugal Pump". Journal of Fluid Machinery. February 2015. Vol 18-1. p.65-71. DOI: http://dx.doi.org/10.5293/kfma.2015.18.1.065.

[12] Wang C, Shi W D, Lu W G et al. "Effect and experiment of different blade thickness on stainless steel stamping well pump performance". Transactions of the Chinese Society for Agricultural Machinery. July 2012. Vol 43-7. p.94-99. DOI: http://dx.doi.org/10.6041/j.issn.1000-1298.2012.07.017.

[13] Dai H, Liu H, Ding J, et al. "Effects of impeller outlet width on pressure pulsation in two side chambers of centrifugal pump". Journal of Drainage and Irrigation Machinery Engineering. February 2015. Vol 33-1. p.20-25. DOI: http://dx.doi.org/10.3969/j.issn.1674-8530.14.0057.

[14] Agrawal N, Agrawal K, Mhaske S. "Experimental investigation of rotor-stator interaction in a centrifugal pump with several vaned diffusers". Journal of Turbomachinery. February 1990. Vol 13-1. p.1-6. DOI: http://dx.doi.org/10.1115/1.2927428.

[15] Yang J, Zhang R H, Wang C L, et al. "Calculation method of area ration and volute cross area for centrifugal pump". Chinese Journal of Mechanical Engineering. August 2006. Vol 42-9. p.67-70. DOI: http://dx.doi.org/10.3901/JME.2006.09.067.

APPRECIATION

This study was supported by the National Natural Science Foundation of China (5160091044), National Science and Technology Small and Medium-sized Enterprise Technology Innovation Fundation under Grant No.14C26213201080, the Jiangsu Natural Science Foundation under Grant No.BK20141302, the Key Research and Development Program of Jiangsu under Grant No.BE2015001-2 and No.BE2015119, the Policy Guidance Class in Jiangsu under Grant No.BY2015064-06, and the Funding for the Construction of Dominant Disciplines in Colleges and Universities in Jiangsu under Grant No.PAPD.